Lab on a Chip

PAPER

View Article Online
View Journal | View Issue

Cite this: *Lab Chip*, 2016, **16**, 353

Optofluidic FRET lasers using aqueous quantum dots as donors†

Qiushu Chen,[a] Alper Kiraz*[ab] and Xudong Fan*[a]

Received 21st August 2015,
Accepted 30th November 2015

DOI: 10.1039/c5lc01004g

www.rsc.org/loc

An optofluidic FRET (fluorescence resonance energy transfer) laser is formed by putting FRET pairs inside a microcavity acting as a gain medium. This integration of an optofluidic laser and the FRET mechanism provides novel research frontiers, including sensitive biochemical analysis and novel photonic devices, such as on-chip coherent light sources and bio-tunable lasers. Here, we investigated an optofluidic FRET laser using quantum dots (QDs) as FRET donors. We achieved lasing from Cy5 as the acceptor in a QD–Cy5 pair upon excitation at 450 nm, where Cy5 has negligible absorption by itself. The threshold was approximately 14 μJ mm^{-2}. The demonstrated capability of QDs as donors in the FRET laser greatly improves the versatility of optofluidic laser operation due to the broad and large absorption cross section of the QDs in the blue and UV spectral regions. The excitation efficiency of the acceptor molecules through a FRET channel was also analyzed, showing that the energy transfer rate and the non-radiative Auger recombination rate of QDs play a significant role in FRET laser performance.

Introduction

Optofluidic lasers have recently emerged as an enabling tool that integrates optical microresonators with microfluidic channels and different gain media in liquid form.[1,2] Optofluidic lasers have great potential in sensitive biochemical detection due to their capability to amplify small changes in analyte emission intensities caused by underlying concentration changes or conformational changes in biomolecules.[3–6] They are also promising for novel on-chip photonic devices, such as on-chip coherent light sources and bio-tunable lasers.[1,2,7–9] An optofluidic laser is usually excited by tuning an external pump laser (such as optical parametric oscillator – OPO) directly into a gain medium absorption band. Alternatively, it can also be excited indirectly using fluorescence resonance energy transfer (FRET), where an acceptor laser can be achieved by excitation funneled from donor molecules through a FRET channel.[6–9] FRET is a widely used technology in biological research to sensitively analyze biomolecules, as the Förster distance of a FRET pair is around 5–10 nm, which is close to the characteristic dimensions of a biomolecule. Incorporating FRET with an optofluidic laser will lead to a number of new research frontiers. On one hand, an optofluidic FRET laser that measures the FRET process inside a laser cavity using laser outputs provides a means to analyze biomolecules with sensitivities orders of magnitude higher than traditional fluorescence-based FRET detection, as recently shown experimentally and theoretically.[6,10,11] On the other hand, FRET significantly enhances the versatility and flexibility of an optofluidic laser by providing another pump mechanism that can extend the optofluidic laser spectral coverage and increase the pumping efficiency.[12] In addition, it enables precise control and modulation of the optofluidic laser *via* biomolecular interactions.[8]

In the past few years, a wide variety of biochemically related fluorophores have been explored as optofluidic laser gain media, including organic dyes,[3,11] biomaterials (fluorescent proteins,[10,13,14] vitamins,[15] luciferins[16]) and products of enzyme–substrate reactions,[5] many of which can also work as the donor or the acceptor in an optofluidic FRET laser.[10,11,16] Semiconductor colloidal quantum dots (QDs) are another type of fluorophore possessing unique photo-physical properties such as color tunability by size, high brightness and good photostability that are of great importance for the development of optofluidic laser technology.[17–20] In particular, due to their high light absorption capability in the blue and UV regions, QDs can collect excitation light more efficiently, resulting in a significantly lower lasing threshold.[20] More recently, optofluidic lasers using biocompatible QDs in an aqueous environment have been demonstrated, paving the way to actual biochemical applications with optofluidic QD lasers.[18,20] In addition to directly acting as the gain medium, QDs have the potential to work as the donor in a FRET laser.

[a] *Department of Biomedical Engineering, University of Michigan, Ann Arbor, MI 48109, USA. E-mail: akiraz@ku.edu.tr, xsfan@umich.edu*
[b] *Department of Physics, Koç University, Rumelifeneri Yolu, Sariyer, 34450 Istanbul, Turkey*

† Electronic supplementary information (ESI) available. See DOI: 10.1039/c5lc01004g

In fact, in the context of traditional fluorescence-based detection, QDs have been extensively studied as the donor[21–26] or acceptor[27] in a FRET pair for various biosensing applications. QDs are especially well suited as donors due to their broad absorption bands, tunable emission bands for controllable spectral overlap with acceptors, and large Stokes shifts for suppression of direct excitation of acceptors.[28,29] However, despite extensive studies of QDs in fluorescence-based FRET, to date, the performance of QDs in an optofluidic FRET laser has rarely been explored.[30]

In this work, we developed and studied an optofluidic QD FRET laser using commercial water-soluble QDs (donor) and dye molecules (acceptor) as a model system. We showed that QDs can assist acceptor dye lasing with an excitation wavelength far from the dye absorption band thanks to FRET. We also investigated the efficiency of our QD FRET laser in comparison with a directly excited dye laser and revealed that the limiting factors for the FRET laser performance are the FRET energy transfer rate and non-radiative Auger recombination. This study has multiple implications. First, to the best of our knowledge, it is the first demonstration of a FRET laser using aqueous QDs as the donor. The integration of optofluidic laser technology with QD FRET that is conceptually demonstrated here has great potential in building ultra-sensitive, versatile and robust platforms for biochemical sensing applications. QDs, with their unique photo-physical properties, are expected to improve the performance of optofluidic FRET lasers and bridge the gap between laboratory technology and real applications. Second, the role of QDs in FRET lasers is of general scientific interest. Optofluidic QD FRET laser studies can also be instrumental in understanding the photophysical properties of QDs as the laser gain medium and as the donor, and in revealing their similarity to and dissimilarity from organic dyes in FRET processes, which is why it will be important for us to take advantage of QDs and overcome their limitations.

Experimental

Water-soluble QDot 655 (Invitrogen) and Cy5 were chosen to be the FRET donor and acceptor in this work. QDot 655 has an organic PEG coating that has active amino groups on the surface. Its emission peak is centered at 655 nm, which has significant overlap with the Cy5 absorption band. Cy5 was purchased from Sigma-Aldrich, which has an NHS ester that can react with amines for labeling (Cy5 NHS ester). In addition, Cy5 labeled on a DNA (Cy5–DNA) was purchased from Integrated DNA Technologies, which served as the negative control in our studies. The reason for using Cy5–DNA instead of pure Cy5 is that Cy5–DNA can dissolve in PBS buffer much more efficiently than pure Cy5.

A covalent immobilization method was used to link the Cy5 NHS ester to the QD surface, which, along with the sample characterization, is described as follows. After changing the buffer of QDot 655 from the original borate buffer to PBS with a 100K Amicon Ultra-0.5 centrifugal filter, 100 μL of 6.25 μM QDot 655 was mixed with 150 μg of Cy5 NHS ester and incubated for 1 h. Then, the mixture was filtered with a resin column that separates free Cy5 NHS ester from a QD–Cy5 conjugate. Multiple tests were performed to characterize the resulting sample. According to the absorption test using a NanoDrop 2000c UV-Vis spectrophotometer (Fig. 1(A)), the concentration of QD and Cy5 was calculated to be 3.3 μM and 29 μM, respectively, corresponding to a labeling ratio of 9 (*i.e.*, 9 Cy5 molecules are covalently linked to one QD on average). The existence of FRET in the QD–Cy5 conjugate was verified by photoluminescence excitation (PLE) conducted with a FluoroMax-4 spectrofluorometer, in which the emission intensity at 720 nm from Cy5 was monitored while scanning the excitation wavelength from 400 nm to 690 nm. A similar pattern was observed in the PLE spectrum compared to the absorption spectrum, as shown in Fig. 1(B), indicating that the photons absorbed by the QDs can be transferred to the Cy5 emission through FRET. The emission spectrum in Fig. 1(C) further shows a peak centered around 665 nm, red-shifted from the original QD peak at 655 nm, which is due to the combination of contributions from QDs and Cy5 upon excitation at 430 nm, where Cy5 has negligible absorption. Further clues for FRET can be derived from lifetime measurements. The measured lifetime of the original QDot 655 sample is 34.6 ns (Fig. S1 and Table S1†). In the conjugate

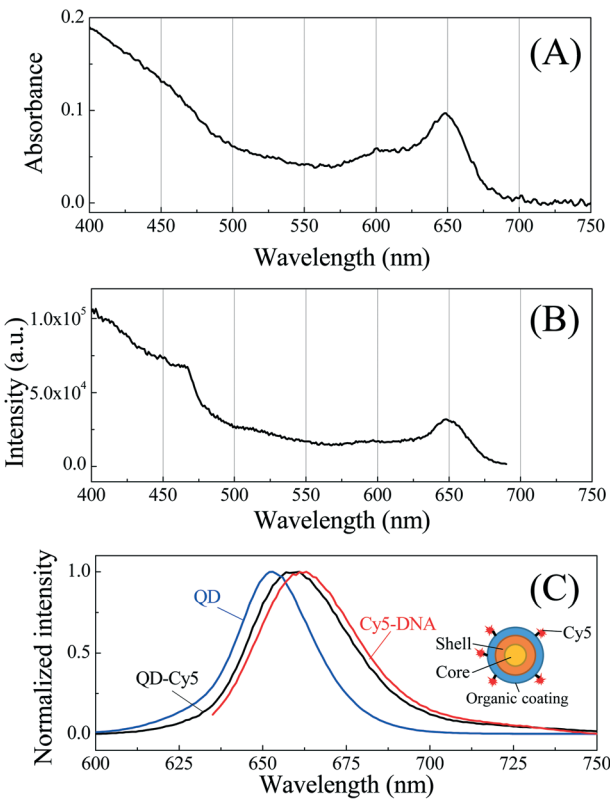

Fig. 1 Characterization of the Cy5-conjugated QD sample. (A) 1 mm absorbance of 10× diluted sample. (B) Photoluminescence excitation spectrum of the same sample in (A). Emission was collected at 720 nm. (C) Normalized emission spectra of pure QD, QD–Cy5 conjugate and Cy5. Inset: a QD–Cy5 conjugate.

sample, the QDot 655 lifetime is significantly reduced to 4.4 ns, indicating the existence of a fast FRET decay channel. A FRET efficiency of 87% can be calculated from the reduced lifetime of QDs in the conjugate sample (see details in the ESI†).

For optofluidic laser studies, we used a capillary-based optofluidic ring resonator (OFRR) as the platform due to its high quality factor optical resonances, simple fabrication and intrinsic microfluidic characteristics for easy sample delivery.[31,32] The OFRR had an outer diameter of approximately 100 μm and a wall thickness of a few micrometers. The circular cross-section of the OFRR supports the whispering gallery mode (WGM) that circulates along its circumference. Due to the thin wall (a few micrometers), the WGM has a sufficient evanescent field in the core and provides optical feedback for the gain medium flowing inside the capillary to lase.[7,32] The preparation of the OFRR was described elsewhere.[31–33] A typical confocal setup was used to excite the sample and collect emission light (Fig. 2). A pulsed OPO laser (pulse width: 5 ns, repetition rate: 20 Hz) was used as the excitation source. The pump intensity was adjusted by a continuously variable neutral density filter. The laser beam was focused on the OFRR using a 20 mm lens. The emission light was collected through the same lens and sent to the spectrometer (Horiba iHR550) for analysis.

Results and discussion

As a control experiment, we first ran a 30 μM Cy5–DNA sample in PBS buffer in the system and studied its lasing performance, which had almost the same Cy5 concentration as the QD–Cy5 conjugate sample. Upon excitation at 450 nm, no lasing could be observed within the system excitation power capability (up to 550 μJ mm^{-2}). As exemplified in the red curve in Fig. 3(A), only a featureless emission spectrum was observed. In contrast, when the QD–Cy5 conjugate sample was flowed through the same capillary immediately after the experiments with Cy5–DNA, Cy5 lasing peaks emerged around 730 nm (Fig. 3(A), black curves) with excitation at the same wavelength (450 nm). The measured linewidth of the lasing peaks was 0.32 nm, which is much sharper than the fluorescence emission. This linewidth is limited by the resolution of our spectrometer (0.05 nm with 600 g mm^{-1} grating)

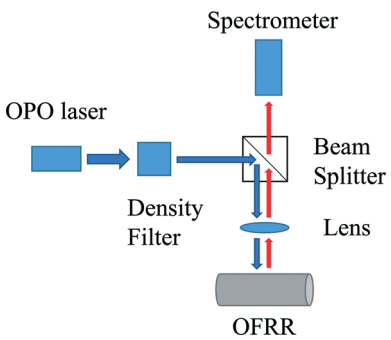

Fig. 2 Optofluidic laser experiment setup.

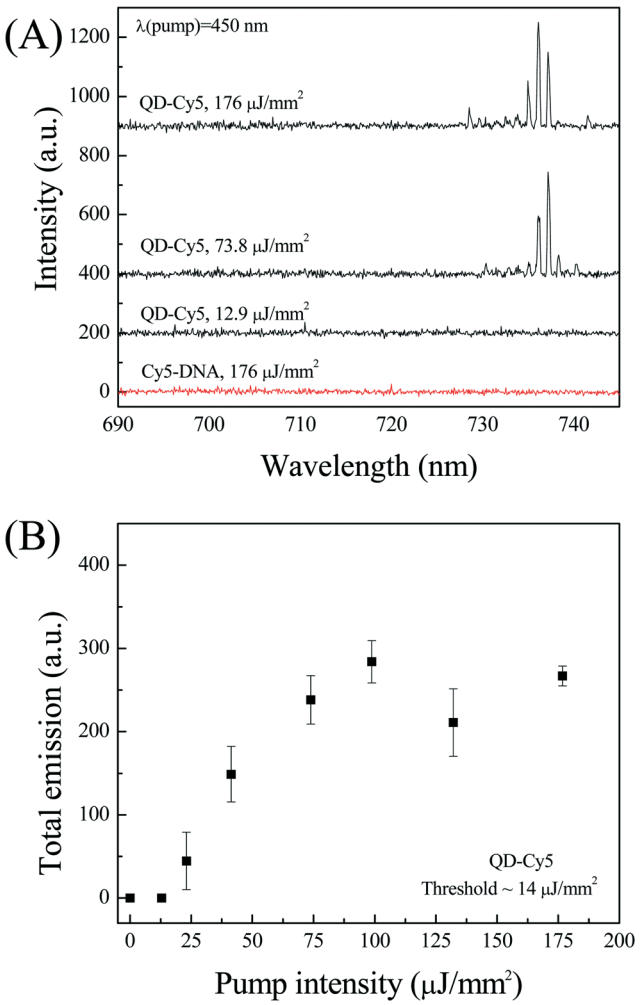

Fig. 3 (A) Emission spectra of QD–Cy5 and Cy5 when pumped at 450 nm. Spectra are vertically shifted for clarity. (B) Spectrally integrated emission *versus* pump intensity for QD–Cy5 when pumped at 450 nm. Spectral integration takes place in the range of 730–740 nm. The lasing threshold for QD–Cy5 is approximately 14 μJ mm^{-2}. Each data point was collected upon single pulse excitation in order to minimize photobleaching. Error bars are obtained with 3 measurements. Concentration of Cy5 in QD–Cy5 in (A) and (B) was 29 μM.

and by the fact that each peak may contain multiple lasing modes that have slightly different lasing wavelengths. The red shift of the lasing peak relative to the fluorescence emission peak of Cy5 is typical for dye lasers,[32] caused by the self-absorption of Cy5 and additional absorption of QDs. Fig. 3(B) plots the Cy5 laser output as a function of pump intensity. A threshold pump intensity of 14 μJ mm^{-2} is derived by fitting the lasing output above the threshold. Beyond the threshold, the Cy5 lasing emission increases linearly with the increase in pump intensity, but levels off when the pump intensity is above 100 μJ mm^{-2}, which indicates saturation in excitation. From these measurements, it can be concluded that through conjugation with QDs, which has strong absorption around 450 nm, Cy5 lasing emission can be achieved *via* FRET.

We further performed a photostability experiment of FRET lasing with the QD–Cy5 sample. Fixing the pump intensity at

176 μJ mm^{-2}, we recorded the lasing spectrum and derived the lasing and fluorescence intensities from different spectral regions over 49 consecutive excitation pulses (Fig. 4(A) and (B)). After 49 excitation pulses, the fluorescence intensity experienced a decrease of less than 20% while a 50% decrease was recorded for lasing emission. This result is consistent with the non-linear nature of the laser mechanism.[34] The relatively rapid photo-bleaching of Cy5 laser emission is due to the high excitation intensity used in the experiment. In contrast, when a lower excitation intensity (36.7 μJ mm^{-2}) was applied, significantly improved photostability was observed (Fig. 4(C) and (D)). In practice, the laser does not need to be operated in high excitation intensity for biosensing. In fact, single pulse excitation at an intensity slightly above the threshold is sufficient.

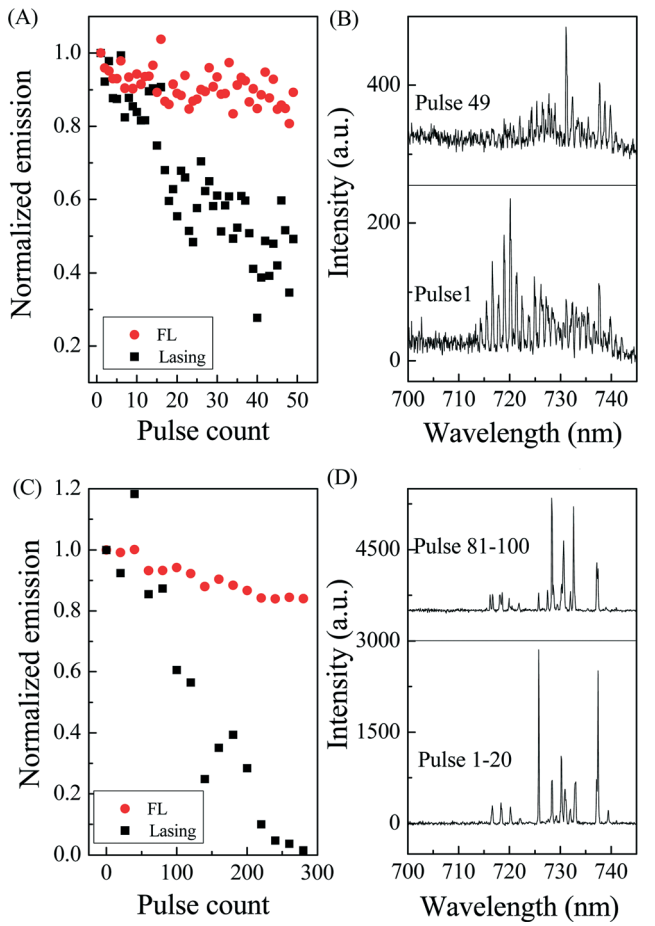

Fig. 4 QD–Cy5 FRET lasing stability study. (A) Normalized spectrally integrated emission for Cy5 fluorescence (675–705 nm) and Cy5 lasing (710–740 nm) under 176 μJ mm^{-2} excitation. Each data point represents the normalized emission under excitation of a single pulse. (B) The corresponding Cy5 laser emission spectrum for the 1st and 49th excitation pulse. (C) Normalized spectrally integrated emission for Cy5 fluorescence (690–700 nm) and Cy5 lasing (710–740 nm) under 36.7 μJ mm^{-2} excitation. Each data point represents the normalized emission under excitation of 20 pulses. (D) The corresponding Cy5 laser emission spectrum for the sum of the 1st–20th pulses and the sum of the 81st–100th excitation pulses.

In general, the equations for the acceptor laser are given as follows:[6]

$$\frac{dn_d}{dt} = I_p\sigma_{d,a}(N_d - n_d) - \frac{n_d}{\tau_d} - k_F n_d \quad (1)$$

$$\frac{dn_a}{dt} = k_F n_d - \frac{n_a}{\tau_a} \quad (2)$$

$$\frac{dq_a}{dt} = \frac{c}{m}\sigma_{a,e}(\lambda_L)n_a - \frac{c}{m}\sigma_{a,a}(\lambda_L)(N_a - n_a) - \frac{q_a}{\tau_{cavity}} \quad (3)$$

where n_d and n_a are the donor and acceptor concentrations in the excited state, respectively. N_d and N_a are the total concentrations for the donor and acceptor, respectively. q_a is the photon number density in the cavity emitted by the acceptor. τ_d, τ_a and τ_{cavity} are the lifetimes of the donor, the acceptor and the photons in the cavity mode. τ_{cavity} is related to the empty cavity Q-factor, Q_0, by $\tau_{cavity} = \frac{Q_0\lambda}{2\pi c}$, where c is the light speed in vacuum. k_F is the energy transfer rate from the donor to the acceptor. $\sigma_{d,a}$, $\sigma_{a,e}$ and $\sigma_{a,a}$ are the donor absorption cross-section, the acceptor emission cross-section and the acceptor absorption cross-section, respectively. I_p is the pump intensity. m is the refractive index of the cavity mode. λ_L is the lasing wavelength. Eqn (1) and (2) describe the donor and acceptor concentrations in the excited state, respectively, whereas eqn (3) describes the number density of photons inside the cavity. Under steady-state conditions, we have:

$$n_d = \frac{I_p\sigma_{d,a}}{I_p\sigma_{d,a} + 1/\tau_d + k_F} N_d \quad (4)$$

$$n_a = \tau_a k_F n_d \quad (5)$$

$$\sigma_{a,e}(\lambda_L)n_a - \sigma_{a,a}(\lambda_L)(N_a - n_a) - \frac{2\pi m}{Q_0\lambda_L} = 0 \quad (6)$$

Eqn (6) leads to the threshold condition for the acceptor concentration, $n_{a,th}$, which is

$$\gamma_{th} = \frac{n_{a,th}}{N_a} \approx \frac{\sigma_{a,a}(\lambda_L)N_a + 2\pi m/(Q_o\lambda_L)}{N_a\sigma_{a,e}(\lambda_L)}. \quad (7)$$

For the case where QDs are used as the donor, eqn (1) may need to be modified to reflect multi-exciton excitation and extremely fast relaxation processes of multi-excitons,[35,36] which are on the order of tens to hundreds of picoseconds, shorter than the energy transfer time ($1/k_F$) of a few nanoseconds. To further understand the energy transfer between the QD donor and the dye acceptor, we chose QDot 655 and Alexa Fluor 680 (AF680) as another donor/acceptor pair. Due to the

smaller spectral overlap between QDot 655 and AF680 (see Fig. S2 in the ESI†), the energy transfer efficiency is lower than that for QDot 655 and Cy5 (see Fig. S3 in the ESI†). Therefore, only distinct fluorescence peaks of the donor and the acceptor were observed using exactly the same experimental conditions as those in the case of QD–Cy5, as plotted in the inset of Fig. 5, which allows us to study the energy transfer between the QD donor and dye acceptor without interference from the acceptor laser emission.

Fig. 5 plots the fluorescence from both QDot 655 and AF680 measured simultaneously with various pump intensities. Initially, the fluorescence from both QDot 655 and AF680 increases concomitantly and is linearly proportional to the pump intensity, indicating that more QDs are excited through direct excitation and more AF680 are excited through FRET. Between 10 and 100 μJ mm^{-2}, QD emission starts to show a certain degree of saturation, *i.e.*, its intensity still grows with the increased pump intensity, but with a smaller slope. Accordingly, AF680 emission has a similar pattern of saturation. When the pump intensity is above 100 μJ mm^{-2}, the QD emission completely levels off, suggesting that no more photons can be emitted by the QDs despite the increased pump intensity. Meanwhile, the AF680 emission still increases with the pump intensity but with a relatively small slope. Detailed analysis in Fig. S4 in the ESI† shows that this slight increase in AF680 emission results from the small direct excitation of AF680 at 450 nm, whereas the emission of AF680 through the energy transfer from the QDs should completely saturate, as suggested by the QD emission. Indeed, after the correction for the emission from the direct excitation, the AF680 emission exhibits the corresponding saturation behavior that follows that in the QD emission (see Fig. S4†).

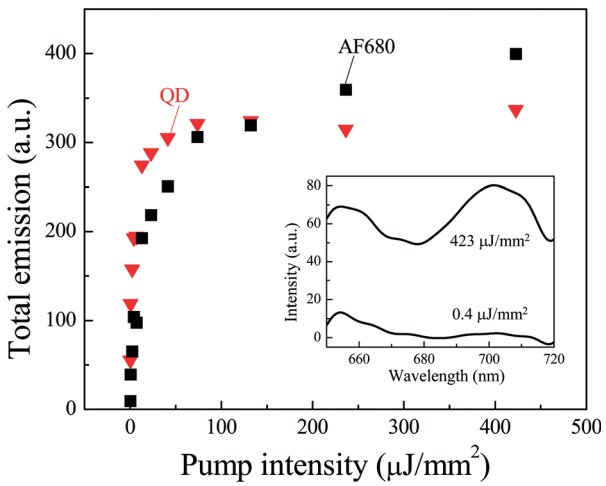

Fig. 5 Spectrally integrated fluorescence of QD and AF680 from QD–AF680 conjugates for various pump intensities at 450 nm. Each data point is recorded under single pulse excitation. Spectral integration takes place in the range of 650–655 nm for QD emission and 700–705 nm for AF680. Inset: emission spectra of QD–AF680 conjugates at different pump intensities. Spectral curves are smoothed with a low pass filter having a cutoff at 0.1 Hz.

The detailed microscopic mechanism of FRET using QDs as the donor can be understood as follows. Upon excitation of multiple excitons, they relax very rapidly down to biexcitons and then to single excitons through non-radiative recombination.[35,36] Since those relaxation processes are very fast in comparison with the radiative decay, they do not contribute to photon generation. The QD fluorescence emission in Fig. 5 comes mainly from biexcitons and single excitons, whose radiative decay rates are comparable to the corresponding non-radiative rates. Both biexcitons and single excitons are able to transfer excitation energy to the acceptor dye.[26] The energy transfer efficiency for biexcitons and single excitons can be written as $\tau_{FRET}^{-1}/(\tau_{FRET}^{-1} + \tau_x^{-1})$, where τ_x is the biexciton ($x = 2$) and single exciton ($x = 1$) lifetime and τ_{FRET} is the energy transfer time. However, since the biexciton lifetime (<2 ns)[26] is much shorter than that of the single exciton (~34 ns) and the energy transfer time for biexcitons and single excitons is similar,[26] the emission from AF680 comes mainly from the energy transferred from single excitons. The same argument is valid for the QD–Cy5 system, whose energy transfer time is 5 ns. Consequently, n_d in eqn (2) should refer to the concentration of single excitons. At high pump intensity (>100 μJ mm^{-2}), we can assume that the concentration of single excitons is the same as the QD concentration. At relatively low pump intensity (<100 μJ mm^{-2}), the fractional single exciton concentration can be deduced by comparing the AF680 fluorescence at low pump intensity with the saturation fluorescence. Based on the above discussion, for the QD–Cy5 conjugates, the lasing threshold of 14 μJ mm^{-2} corresponds to an n_d of 2 μM (=3.3 μM × 0.6, where 0.6 is the ratio of AF680 fluorescence between 14 μJ mm^{-2} and 100 μJ mm^{-2}). Using τ_a = 1 ns for Cy5 and $k_F = (5\ \text{ns})^{-1}$ in eqn (5), we arrive at n_a = 0.4 μM and $\gamma = n_a/N_a$ = 1.4%. At high pump intensity, the Cy5 laser emission saturates beyond 100 μJ mm^{-2}, consistent with the QD saturation behavior obtained by fluorescence measurement using QD–AF680.

To further examine the γ value, we performed laser measurement using Cy5–DNA under exactly the same conditions as those in the case of QD–Cy5, except that the pump wavelength was moved to 500 nm where Cy5 has much higher absorption than at 450 nm. Fig. 6 shows that lasing emission can be achieved with a threshold of approximately 13 μJ mm^{-2}. For direct excitation, the concentration of Cy5 at the excited state can be calculated by:

$$n_a = \frac{I_p \sigma_{a,a}(500\ \text{nm})}{I_p \sigma_{a,a}(500\ \text{nm}) + 1/\tau_a} N_a. \quad (8)$$

Using $\sigma_{a,a} = 0.31 \times 10^{-16}$ cm^2 at 500 nm (see Fig. S1 or Table S1†), τ_a = 1 ns and $I_p = 6.5 \times 10^{14}$ cm^{-2} ns^{-1}, we obtain $\gamma = n_a/N_a$ = 2.0%, which has the same level of Cy5 excitation as in the QD–Cy5 conjugates. Furthermore, in eqn (7), using $\sigma_{a,e} = 2.5 \times 10^{-16}$ cm^2, $Q_0 = 2 \times 10^6$, λ_L = 730 nm and ignoring the first term (*i.e.*, $\sigma_{a,a}N_a$, as it is small compared to the second

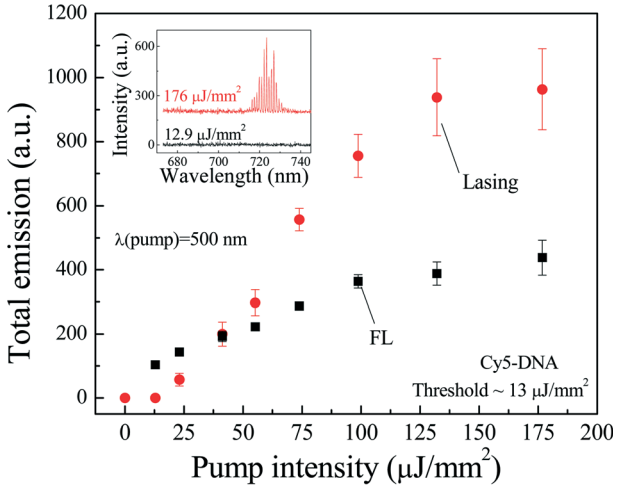

Fig. 6 Spectrally integrated emission *versus* pump intensity for Cy5 when pumped at 500 nm. Spectral integration takes place in the range of 715–735 nm for lasing and 680–700 nm for fluorescence (FL). Inset: emission spectrum of Cy 3 pumped at 176 μJ mm^{-2}. The lasing threshold for Cy5 is approximately 13 μJ mm^{-2}. Concentration of Cy5 was 30 μM. Experimental conditions were the same as those in Fig. 3.

term related to the cavity loss), we obtain the lasing threshold conditions of $n_{a,th}$ = 0.41 μM and γ_{th} = 1.4%.

From our experimental results and theoretical analysis, we conclude that there are two major strategies to achieve a FRET laser with QDs as the donor. The first one is to increase the FRET energy transfer rate k_F (see eqn (5)). This can be fulfilled by (1) choosing a good FRET pair in which the emission band of QDs has significant overlap with the acceptor absorption band, (2) carefully tuning the distance between the core of the quantum dots and the acceptor to enable sufficient energy transfer and (3) increasing the labeling ratio. The second strategy is to suppress the non-radiative Auger recombination rate of multi-exciton states of QDs to enable FRET from higher-order exciton states. For this purpose, QDs with better surface chemical designs or type II QDs can be used[37–40] to further exploit the large absorption cross-section of QDs in FRET lasing.

Conclusion

In summary, we have investigated the capability of QDs as the donor for optofluidic FRET laser operation and successfully achieved lasing from acceptor molecules in a QD–Cy5 system upon excitation at 450 nm where Cy5 has negligible absorption by itself, thus significantly extending the excitation spectral range for the acceptor. The lasing threshold was approximately 14 μJ mm^{-2}. The power-dependent fluorescence and laser studies suggest that the excitation of the acceptor comes mainly from the energy transferred from single excitons in QDs. We further reveal the similarities and dissimilarities between organic dyes and QDs as the donor and point out the methods to improve optofluidic FRET laser performance when QDs are used as the donor.

Acknowledgements

The authors acknowledge the support from the National Institutes of Health (1R21EB016783). A. K. acknowledges the support from Fulbright Fellowship and the University of Michigan as a visiting scholar. The authors also thank M.-A. Mycek for the QD lifetime measurement and S. Sivaramakrishnan for the help in sample preparation and characterization.

References

1 Z. Li and D. Psaltis, Optofluidic dye lasers, *Microfluid. Nanofluid.*, 2008, **4**, 145–158.
2 X. Fan and S. H. Yun, The potential of optofluidic biolasers, *Nat. Methods*, 2014, **11**, 141–147.
3 W. Lee and X. Fan, Intracavity DNA melting analysis with optofluidic lasers, *Anal. Chem.*, 2012, **84**, 9558–9563.
4 Y. Sun and X. Fan, Distinguishing DNA by Analog-to-Digital-like Conversion by Using Optofluidic Lasers, *Angew. Chem., Int. Ed.*, 2012, **51**, 1236–1239.
5 X. Wu, M. K. K. Oo, K. Reddy, Q. Chen, Y. Sun and X. Fan, Optofluidic laser for dual-mode sensitive biomolecular detection with a large dynamic range, *Nat. Commun.*, 2014, **5**, 3779.
6 M. Aas, Q. Chen, A. Jonáš, A. Kiraz and X. Fan, Optofluidic FRET Lasers and Their Applications in Novel Photonic Devices and Biochemical Sensing, *IEEE J. Sel. Top. Quantum Electron.*, 2016, **22**, 7000215.
7 Y. Sun, S. I. Shopova, C.-S. Wu, S. Arnold and X. Fan, Bioinspired optofluidic FRET lasers via DNA scaffolds, *Proc. Natl. Acad. Sci. U. S. A.*, 2010, **107**, 16039–16042.
8 Q. Chen, H. Liu, W. Lee, Y. Sun, D. Zhu, H. Pei, C. Fan and X. Fan, Self-assembled DNA tetrahedral optofluidic lasers with precise and tunable gain control, *Lab Chip*, 2013, **13**, 3351–3354.
9 M. Aas, E. Ozelci, A. Jonas, A. Kiraz, H. Liu, C. Fan, Q. Chen and X. Fan, FRET lasing from self-assembled DNA tetrahedral nanostructures suspended in optofluidic droplet resonators, *Eur. Phys. J. A*, 2014, **223**, 2057–2062.
10 Q. Chen, X. Zhang, Y. Sun, M. Ritt, S. Sivaramakrishnan and X. Fan, Highly sensitive fluorescent protein FRET detection using optofluidic lasers, *Lab Chip*, 2013, **13**, 2679–2681.
11 X. Zhang, W. Lee and X. Fan, Bio-switchable optofluidic lasers based on DNA Holliday junctions, *Lab Chip*, 2012, **12**, 3673–3675.
12 L. Cerdan, E. Enciso, V. Martin, J. Banuelos, I. Lopez-Arbeloa, A. Costela and I. Garcia-Moreno, FRET-assisted laser emission in colloidal suspensions of dye-doped latex nanoparticles, *Nat. Photonics*, 2012, **6**, 621–626.
13 M. C. Gather and S. H. Yun, Single-cell biological lasers, *Nat. Photonics*, 2011, **5**, 406–410.
14 M. C. Gather and S. H. Yun, Bio-optimized energy transfer in densely packed fluorescent protein enables near-maximal luminescence and solid-state lasers, *Nat. Commun.*, 2014, **5**, 5722.
15 S. Nizamoglu, M. C. Gather and S. H. Yun, All-biomaterial laser using vitamin and biopolymers, *Adv. Mater.*, 2013, **25**, 5943–5947.

16 X. Wu, Q. Chen, Y. Sun and X. Fan, Bio-inspired optofluidic lasers with luciferin, *Appl. Phys. Lett.*, 2013, **102**, 203706.
17 M. Kazes, D. Y. Lewis, Y. Ebenstein, T. Mokari and U. Banin, Lasing from semiconductor quantum rods in a cylindrical microcavity, *Adv. Mater.*, 2002, **14**, 317–321.
18 J. Schäfer, J. P. Mondia, R. Sharma, Z. H. Lu, A. S. Susha, A. L. Rogach and L. J. Wang, Quantum Dot Microdrop Laser, *Nano Lett.*, 2008, **8**, 1709–1712.
19 Y. Wang, K. S. Leck, V. D. Ta, R. Chen, V. Nalla, Y. Gao, T. He, H. V. Demir and H. Sun, Blue Liquid Lasers from Solution of CdZnS/ZnS Ternary Alloy Quantum Dots with Quasi-Continuous Pumping, *Adv. Mater.*, 2015, **27**, 169–175.
20 A. Kiraz, Q. Chen and X. Fan, Optofluidic lasers with aqueous quantum dots, *ACS Photonics*, 2015, **2**, 707–713.
21 D. M. Willard, L. L. Carillo, J. Jung and A. V. Orden, CdSe-ZnS quantum dots as resonance energy transfer donors in a model protein-protein binding assay, *Nano Lett.*, 2001, **1**, 469–474.
22 S. Wang, N. Mmedova, N. A. Kotov, W. Chen and J. Studer, Antigen/antibody immunocomplex from CdTe nanoparticle bioconjugates, *Nano Lett.*, 2002, **2**, 817–822.
23 I. L. Medintz, A. R. Clapp, H. Mattoussi, E. R. Goldman, B. Fisher and J. M. Mauro, Self-assembled nanoscale biosensors based on quantum dot FRET donors, *Nat. Mater.*, 2003, **2**, 630–638.
24 C.-Y. Zhang, H.-C. Yeh, M. T. Kuroki and T.-H. Wang, Single-quantum-dot-based DNA nanosensor, *Nat. Mater.*, 2005, **4**, 826–831.
25 A. R. Clapp, I. L. Medintz and H. Mattoussi, Forster resonance energy transfer investigations using quantum-dot fluorophores, *ChemPhysChem*, 2006, **7**, 47–57.
26 J. Xiao, Y. Wang, Z. Hua, X. Wang, C. Zhang and M. Xiao, Carrier multiplication in semiconductor nanocrystals detected by energy transfer to organic dye molecules, *Nat. Commun.*, 2012, **3**, 1170.
27 Y. Wang, L. Bao, Z. Liu and D.-W. Pang, Aptamer biosensor based on fluorescence resonance energy transfer from upconverting phosphors to carbon nanoparticles for thrombin detection in human plasma, *Anal. Chem.*, 2011, **83**, 8130–8137.
28 I. L. Medintz, H. T. Uyeda, E. R. Goldman and H. Mattoussi, Quantum dot bioconjugates for imaging, labelling and sensing, *Nat. Mater.*, 2006, **4**, 435–446.
29 R. C. Somers, M. G. Bawendi and D. G. Nocera, CdSe nanocrystal based chem-/bio-sensors, *Chem. Soc. Rev.*, 2007, **36**, 579–591.
30 S. I. Shopova, J. M. Cupps, P. Zhang, E. P. Henderson, S. Lacey and X. Fan, Opto-fluidic ring resonator lasers based on highly efficient resonant energy transfer, *Opt. Express*, 2007, **15**, 12735–12742.
31 I. M. White, H. Oveys and X. Fan, Liquid Core Optical Ring Resonator Sensors, *Opt. Lett.*, 2006, **31**, 1319–1321.
32 S. I. Shopova, H. Zhou, X. Fan and P. Zhang, Optofluidic ring resonator based dye laser, *Appl. Phys. Lett.*, 2007, **90**, 221101.
33 K. Han, K. H. Kim, J. Kim, W. Lee, J. Liu, X. Fan, T. Carmon and G. Bahl, Fabrication and Testing of Microfluidic Optomechanical Oscillators, *J. Visualized Exp.*, 2014, **87**, e51497.
34 A. Jonáš, M. Aas, Y. Karadag, S. Manioğlu, S. Anand, D. McGloin, H. Bayraktar and A. Kirazb, In vitro and in vivo biolasing of fluorescent proteins suspended in liquid microdroplet cavities, *Lab Chip*, 2014, **14**, 3093–3100.
35 H. Htoon, J. Hollingsworth, R. Dickerson and V. Klimov, Effect of Zero- to One-Dimensional Transformation on Multiparticle Auger Recombination in Semiconductor Quantum Rods, *Phys. Rev. Lett.*, 2003, **91**, 227401.
36 V. I. Klimov, Spectral and Dynamical Properties of Multiexcitons in Semiconductor Nanocrystals, *Annu. Rev. Phys. Chem.*, 2007, **58**, 635–673.
37 Y.-S. Park, A. V. Malko, J. Vela, Y. Chen, Y. Ghosh, F. García-Santamaría, J. A. Hollingsworth, V. I. Klimov and H. Htoon, Near-Unity Quantum Yields of Biexciton Emission from CdSe/CdS Nanocrystals Measured Using Single-Particle Spectroscopy, *Phys. Rev. Lett.*, 2011, **106**, 187401.
38 A. M. Dennis, B. D. Mangum, A. Piryatinski, Y.-S. Park, D. C. Hannah, J. L. Casson, D. J. Williams, R. D. Schaller, H. Htoon and J. A. Hollingsworth, Suppressed blinking and Auger recombination in near-infrared type-II InP/CdS Nanocrystal Quantum Dots, *Nano Lett.*, 2012, **12**, 5545–5551.
39 W. K. Bae, Y.-S. Park, J. Lim, D. Lee, L. A. Padilha, H. McDaniel, I. Robel, C. Lee, J. M. Pietryga and V. I. Klimov, Controlling the influence of Auger recombination on the performance of quantum-dot light-emitting diodes, *Nat. Commun.*, 2013, **4**, 2661.
40 Y.-S. Park, W. K. Bae, L. A. Padilha, J. M. Pietryga and V. I. Klimov, Effect of the core/shell interface on Auger recombination evaluated by single-quantum-dot spectroscopy, *Nano Lett.*, 2014, **14**, 396–402.